JCIM JOURNAL OF CHEMICAL INFORMATION AND MODELING

pubs.acs.org/jcim Article

Pathway-Based Drug Repurposing with DPNetinfer: A Method to Predict Drug−Pathway Associations via Network-Based Approaches

Jiye Wang,[#] Zengrui Wu,[#] Yayuan Peng, Weihua Li, Guixia Liu, and Yun Tang*

Cite This: J. Chem. Inf. Model. 2021, 61, 2475−2485 Read Online

ACCESS | Metrics & More | Article Recommendations | Supporting Information

ABSTRACT: Identification of drug−pathway associations plays an important role in pathway-based drug repurposing. However, it is time-consuming and costly to uncover new drug−pathway associations experimentally. The drug-induced transcriptomics data provide a global view of cellular pathways and tell how these pathways change under different treatments. These data enable computational approaches for large-scale prediction of drug−pathway associations. Here we introduced DPNetinfer, a novel computational method to predict potential drug−pathway associations based on substructure−drug−pathway networks via network-based approaches. The results demonstrated that DPNetinfer performed well in a pan-cancer network with an AUC (area under curve) = 0.9358. Meanwhile, DPNetinfer was shown to have a good capability of generalization on two external validation sets (AUC = 0.8519 and 0.7494, respectively). As a case study, DPNetinfer was used in pathway-based drug repurposing for cancer therapy. Unexpected anticancer activities of some nononcology drugs were then identified on the PI3K-Akt pathway. Considering tumor heterogeneity, seven primary site-based models were constructed by DPNetinfer in different drug−pathway networks. In a word, DPNetinfer provides a powerful tool for large-scale prediction of drug−pathway associations in pathway-based drug repurposing. A web tool for DPNetinfer is freely available at http://lmmd.ecust.edu.cn/netinfer/.

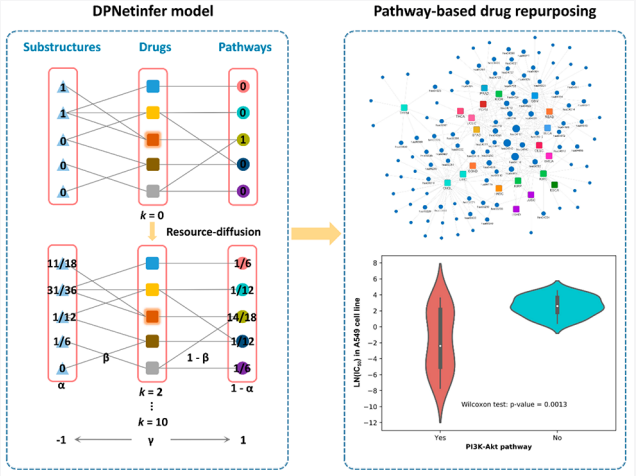

1. INTRODUCTION

The traditional drug discovery paradigm generally follows the classical hypothesis of "one drug → one target → one disease".[1] However, studies have demonstrated that many drugs generally produce therapeutic effects via modulation of multiple proteins or disease-related pathways rather than a single target.[2,3] For example, sorafenib blocked the RAF/MEK/ERK pathway to inhibit tumor progression and angiogenesis.[4] Previous study has identified several pathways as frequent genetic alterations in cancer, mainly including the cell cycle and PI3K-Akt pathways.[5] Furthermore, targeting these pathways involved in disease modification could enable the development of drug candidates with reduced risk of adverse effects.[6] Therefore, biological pathways play an important role in drug discovery.

Recently, a new strategy of drug discovery, namely pathway-based drug discovery, was proposed.[7−9] This strategy mainly identifies drug−pathway associations that drugs act on disease-related pathways by changing the expression of genes in pathways. One recent study showed that pathway-based drug discovery represented an effective strategy to identify potential therapeutic drugs of thoracic aneurysms.[10] However, it is costly and time-consuming to discover new drug−pathway associations experimentally. With the development of multiomics technologies, drug-induced transcriptomics data provide a global view of cellular state (e.g., pathways) and tell how this state changes under different treatments (e.g., drugs).[11] For instance, the Library of Integrated Network-Based Cellular Signatures (LINCS) L1000 database stores gene expression profiles induced by 20 413 compounds on 72 human cell lines.[12] These data enable computational approaches for large-scale prediction of drug−pathway associations.

In previous studies, some computational approaches have been developed to identify potential drug−pathway associations. These methods can be divided into three classes, namely Bayesian spare factor-based,[13,14] matrix decomposition-based,[15] and other machine learning methods.[16] Enrichment analysis and causal inference are also used for pathway-based

Received: January 5, 2021
Published: April 26, 2021

https://doi.org/10.1021/acs.jcim.1c00009
J. Chem. Inf. Model. 2021, 61, 2475−2485

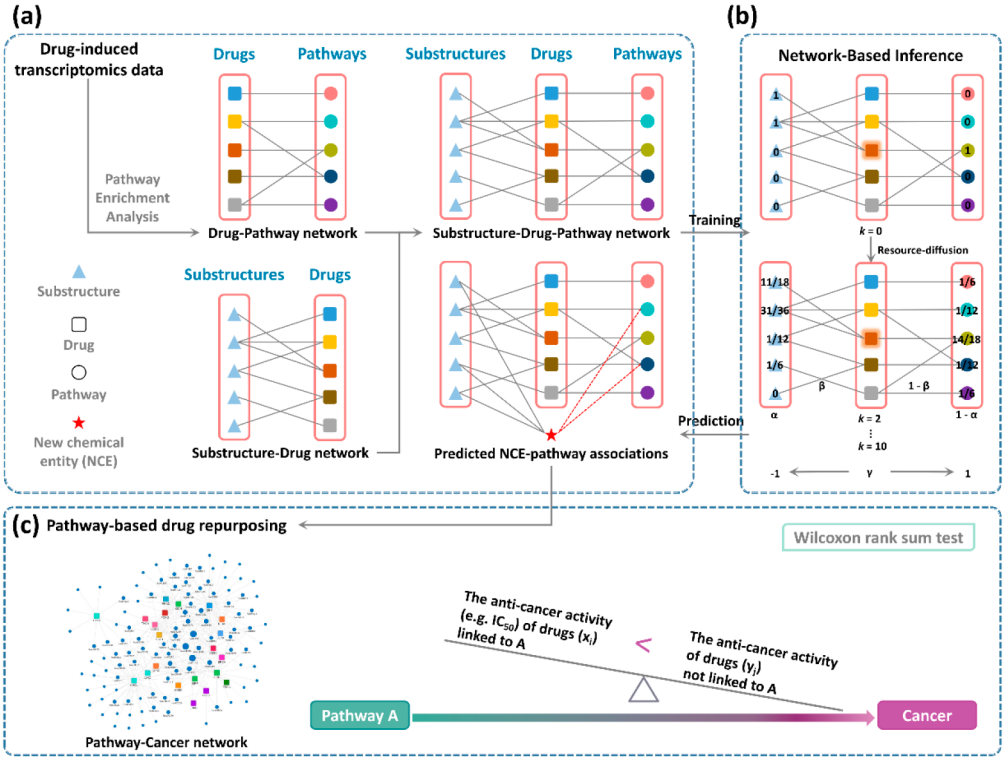

Figure 1. Pipeline of DPNetinfer. (a) Construction of a substructure−drug−pathway network based on drug-induced transcriptomics data. (b) Development of DPNetinfer method on the basis of a substructure−drug−pathway network with bSDTNBI method. (c) Identification of pathway-based drug repurposing for cancer therapy by the DPNetinfer method.

drug discovery.[7,17−19] However, these computational methods can only predict potential pathways for known drugs in existing drug−pathway data sets, rather than for new chemical entities (NCEs). Moreover, it is difficult to obtain negative samples for some supervised machine learning methods.

In recent years, a series of network-based methods have been developed by our group, including network-based inference (NBI),[20] substructure−drug−target NBI (SDTNBI),[21] and balanced SDTNBI (bSDTNBI) methods,[22] which provide important tools for prediction of biological associations.[20−25] Meanwhile, our methods are independent of negative samples, a great advantage over supervised machine learning methods. Furthermore, chemical substructures are used as bridges to link NCEs and known biological networks, which enable prediction of potential biological associations for old drugs, clinically failed drugs, and NCEs in a large scale. Therefore, network-based methods may be used in prediction of potential drug−pathway associations by means of drug-induced transcriptomics data.

In this work, we developed DPNetinfer, a novel computational method to predict potential drug−pathway associations for old drugs, clinically failed drugs, and NCEs. As a case study in pathway-based drug repurposing, we tried to discover anticancer potentials of nononcology drugs using DPNetinfer. The framework of DPNetinfer contains three steps (Figure 1): (a) build substructure−drug−pathway networks based on drug-induced transcriptomics data (Figure 1a), (b) construct the DPNetinfer model on the basis of substructure−drug−pathway networks with bSDTNBI (Figure 1b), and (c) identify pathway-based drug repurposing for cancer therapy by DPNetinfer (Figure 1c). The proposed method was validated by external validation sets and literature, which made us confident that this study could help preclinical research for discovery of more effective anticancer drugs.

2. MATERIALS AND METHODS

2.1. Development of the DPNetinfer Method.

2.1.1. Benchmark Data Sets. The chemical structures of all drugs were converted into canonical SMILES format and standardized by Pipeline Pilot software 2017 R2 (BIOVIA, USA). Only those drugs with 200 ≤ molecular weight ≤800 Da and >3 carbon atoms were selected. The drug−pathway associations were defined by pathway enrichment analysis on drug-induced gene signatures (adjusted p-values < 0.01). The drug-induced transcriptomics data from L1000 fireworks display (L1000FWD) data set[26] were used to construct known drug−pathway networks, which were measured at 6 h in 64 cell lines treated with 4058 drugs (treatment concentration = 10 μM, Table S1). We downloaded up and down gene sets as drug-induced gene signatures by signature ID.

To construct a global drug−pathway network (also called a pan-cancer network) covering all types of cancer (Table S2), the drug-induced gene signatures were merged by the same drugs in all cancer cell lines. In consideration of tumor heterogeneity, these drug-induced gene signatures were merged by the same drug in the same primary site of cell lines. These primary sites mainly included breast, colorectal, kidney, liver, lung, prostate, and skin cancers.

Furthermore, the Affymetrix-based Connectivity Map (CMap) data set (https://portals.broadinstitute.org/cmap/) was considered as an external validation set, which was measured at 6 h, of 3 cell lines treated with 86 drugs (treatment concentration = 10 μM) (Table S3). The drug-

https://doi.org/10.1021/acs.jcim.1c00009
J. Chem. Inf. Model. 2021, 61, 2475−2485

induced gene signatures were calculated by the difference between perturbation and vehicle, which were defined with $|\log_2$ fold-change$| > 1$ in each cell line. The drug-induced gene signatures of external validation set were merged by the same drugs in different cell lines. Finally, different drug−pathway networks were constructed by the pathway enrichment analysis on drug-induced gene signatures.

2.1.2. Description of Substructures. Chemical substructures of all drugs were characterized by molecular fingerprints (FPs) to systematically evaluate the performance of models. In this study, four types of FPs were generated by the PaDEL-Descriptor software (version 2.2.1),[27] including Klekota-Roth (4860 bits), MACCS (166 bits), PubChem (881 bits), and Substructure (307 bits) FPs. Moreover, 1024 and 2048 bits of Morgan FP (radius = 1, 2) were generated by RDKit (https://www.rdkit.org/). In total, five types of FPs for each drug were employed to build models.

2.1.3. Algorithm of DPNetinfer. To describe this method mathematically, three sets were defined as below: (a) the drug set $D = \{D_1, D_2, ..., D_{N_D}\}$, (b) the pathway set $P = \{P_1, P_2, ..., P_{N_P}\}$, and (c) the substructure set $S = \{S_1, S_2, ..., S_{N_S}\}$.

Using these sets, the drug−pathway network was represented as a matrix A_{DP}:

$$A_{DP}(i, j) = \begin{cases} 1 & \text{if } D_i \text{ act on } P_j \\ 0 & \text{otherwise} \end{cases} \quad (1)$$

where $i \in (0, N_D]$, $j \in (0, N_P]$ are positive integers.

The drug−substructure linkages were also represented as a matrix A_{DS}:

$$A_{DS}(i, j) = \begin{cases} 1 & \text{if } D_i \text{ contains } S_j \\ 0 & \text{otherwise} \end{cases} \quad (2)$$

where $i \in (0, N_D]$, $j \in (0, N_S]$ are positive integers.

To eliminate the influence of drugs without known pathways during the resource-diffusion process, two matrices were defined as B_{DP} and B_{DS}:

$$B_{DP}(i, j) = \begin{cases} A_{DP}(i, j) & \text{if } \sum_{l=1}^{N_P} A_{DP}(i, l) \neq 0 \\ 0 & \text{otherwise} \end{cases} \quad (3)$$

where $i \in (0, N_D]$, $j \in (0, N_P]$ are positive integers.

$$B_{DS}(i, j) = \begin{cases} A_{DS}(i, j) & \text{if } \sum_{l=1}^{N_P} A_{DP}(i, l) \neq 0 \\ 0 & \text{otherwise} \end{cases} \quad (4)$$

where $i \in (0, N_D]$, $j \in (0, N_S]$ are positive integers.

With these defined matrices, DPNetinfer performed resource-diffusion process in substructure−drug−pathway network to predict potential drug−pathway associations. Three tunable parameters $\alpha \in [0, 1)$, $\beta \in [0, 1)$, and $\gamma \in [-1, 1]$ were imported into the resource-diffusion process to improve the model performance.

First, two matrices were defined, where parameter α was used to adjust the initial resource allocation of different node types, the equations as follows:

$$A'_{DS}(i, j) = \frac{\alpha A_{DS}(i, j)}{\sum_{l=1}^{N_S} A_{DS}(i, l)} \quad (5)$$

where $i \in (0, N_D]$, $j \in (0, N_S]$ are positive integers.

$$A'_{DP}(i, j) = \frac{(1 - \alpha) A_{DP}(i, j)}{\sum_{l=1}^{N_P} A_{DP}(i, l)} \quad (6)$$

where $i \in (0, N_D]$, $j \in (0, N_P]$ are positive integers.

According to the newly defined matrices, the initial resource matrix (A) can be represented as

$$A = \begin{bmatrix} 0 & A'_{DS} & A'_{DP} \\ A'^{T}_{DS} & 0 & 0 \\ A'^{T}_{DP} & 0 & 0 \end{bmatrix} \quad (7)$$

Then, the transfer matrix of one-step resource diffusion was calculated, where the parameters β and γ were used to adjust the weighted values of different edge types and the influence of hub nodes, respectively. The equations were listed below:

$$B = \begin{bmatrix} 0 & \beta B_{DS} & (1 - \beta) B_{DP} \\ \beta B^{T}_{DS} & 0 & 0 \\ (1 - \beta) B^{T}_{DP} & 0 & 0 \end{bmatrix} \quad (8)$$

$$C(i, j) = B(i, j) \left[\sum_{l=1}^{N_D + N_S + N_P} B(l, j) \right]^{\gamma} \quad (9)$$

$$W(i, j) = \begin{cases} \frac{C(i, j)}{\sum_{l=1}^{N_D + N_S + N_P} C(i, l)} & \text{if } C(i, j) \neq 0 \\ 0 & \text{otherwise} \end{cases} \quad (10)$$

where $i, j \in (0, N_D + N_S + N_P]$ are positive integers.

Let k as the number of resource-diffusion process, the final resource matrix can be calculated by

$$\mathbf{F} = A \times W^k \quad (11)$$

The value of $\mathbf{F}(i, N_D + N_S + j)$ is the predictive score of the association between drug D_i and pathway P_j, where $i \in (0, N_D]$, $j \in (0, N_P]$ are positive integers.

2.1.4. Evaluation of the DPNetinfer Method. 10-fold Cross Validation. For 10-fold cross validation, 10% of drug−pathway associations were randomly separated from the substructure−drug−pathway network as test set in turn. The residual network including the other 90% of drug−pathway associations and all drug−substructure linkages were used as training set. For the sake of reducing the randomness, 10-fold cross validation was repeated 10 times.

Parameter Optimization. Under different conditions including k = 2, 4, 6, 8, 10, and FPs, an approach combining grid search and 10-fold cross validation was used to obtain the optimal values of three parameters (α, β, γ). First, under the assumption of parameter $\gamma = 0$, the optimal values of α and β were searched in the range of $0 \leq \alpha < 1$ and $0 \leq \beta < 1$ with a step length of 0.1. Then, based on the optimal values of α and β, the optimal value of γ was searched in the range of $-1 \leq \gamma \leq 1$ with a step length of 0.1. Finally, the best model was chosen by comparing the performance of models under different conditions.

https://doi.org/10.1021/acs.jcim.1c00009
J. Chem. Inf. Model. 2021, 61, 2475−2485

Calculation of Evaluation Indicators. As mentioned above, the performance of DPNetinfer was evaluated by 10-fold cross validation. Considering the predicted drug−pathway associations in the top-length (L) places for each drug, we chose two L-dependent evaluation indicators including precision (P) and recall (R). With a given L value, higher values of evaluation indicators showed higher model performance. The details of these evaluation indicators were described below:

$$P(L) = \frac{1}{M}\sum_{i=1}^{M}\frac{X_i(L)}{L} \tag{12}$$

$$R(L) = \frac{1}{M}\sum_{i=1}^{M}\frac{X_i(L)}{X_i} \tag{13}$$

where M and N are the numbers of drugs and pathways participated in evaluation, X_i is the number of missing drug−pathway associations of drug D_i, and $X_i(L)$ is the number of true-positive predictions (i.e., missing drug−pathway associations recovered correctly) ranked in the top-L places of the predicted pathway list of drug D_i. In addition, a receiver operating characteristic curve (ROC) was generated for each training−test pair by computing a series of true positive and false positive rates under different L (L = 1, 2, ... N), and the area under curve (AUC) was calculated. For a model, higher AUC values in cross validations usually mean higher ability of distinguishing positive drug−pathway associations from all possible drug−pathway associations.[28] Finally, the model performance was represented by the mean value and standard deviation (mean ± SD) of each evaluation indicator.

Generalization Ability of Model. The model generalization ability was evaluated by two external validation sets. Due to the limitation of available drug-induced transcriptomics data, 20% of the drugs and their drug−pathway associations were randomly separated from the pan-cancer network as external validation set 1 (Table S4). The drug−pathway network from the Affymetrix-based CMap data set was considered as external validation set 2 (Table S4). After inferring potential drug−pathway associations, evaluation indicators were calculated and further characterized as model generalization ability by comparing prediction drug−pathway associations with known drug−pathway associations.

2.2. Case Study: Pathway-Based Drug Repurposing.

2.2.1. Data Collection and Preparation. To explore the anticancer efficacy of nononcology drugs by pathway-based drug repurposing, the pathway−cancer network was constructed to analyze the critical role of pathways in cancer (Figure 1c). First, the transcriptome profiling was downloaded from The Cancer Genome Atlas (TCGA) data portal (https://portal.gdc.cancer.gov/), containing RNA-Seq (read counts) data of 8628 samples from 21 tumor types (Table S5). Then, we performed analysis of differential expression genes (DEGs) with DESeq2 package.[29] These genes with $|\log_2$ fold-change$|$ > 1 and adjusted p-values < 0.05 (Benjamini−Hochberg method) were considered as significant DEGs. Finally, the pathway−cancer network was constructed by pathway enrichment analysis for each tumor type. The Cytoscape NetworkAnalyzer plugin[30] was applied to further analyze the key pathway nodes in the pathway−cancer network.

2.2.2. Prediction of Drug−Pathway Association with DPNetinfer. The DPNetinfer method was used to predict potential pathways for each drug. It was assumed that if a drug acted on one cancer-related pathway (e.g., pathway A), the drug could be a potential anticancer drug (Figure 1c). The Wilcoxon rank sum test (one-sided) was used to calculate the statistical significance of pathway A. The alternative hypothesis was supposed that the anticancer activity (e.g., IC_{50}) of a drug (x_i) linked to pathway A could be better than that of another drug (y_j) not linked to pathway A. To test this hypothesis, the IC_{50} values were collected from the *Journal of Medicinal Chemistry*,[31−33] including 46 NCEs on the A549 cell line (Table S6). Potential drug−pathway associations of these NCEs were predicted by the DPNetinfer method. Subsequently, pathway-based characterization of anticancer drugs was analyzed by Wilcoxon rank sum test. In addition, 24 known anticancer drugs from the CCLE database[34] were predicted by the DPNetinfer method (Table S7).

According to the above proposed pathway-based characterization of anticancer drugs, we tried to discover the anticancer potentials of nononcology drugs. Approved drugs from DrugBank[35] were divided into anticancer drugs, nononcology drugs, and unclear-category drugs according to the first-level of anatomical therapeutic chemical (ATC) codes (L01-antineoploastic agents) (Table S8). Potential drug−pathway associations of approved drugs were predicted and further analyzed by the DPNetinfer method.

2.2.3. Pathway Enrichment Analysis. The KEGG pathway enrichment analysis was performed on drug-induced gene signatures and DEGs of different tumor types by R package clusterProfiler.[36] It should be noted that the biological pathways were filtered in this study. We selected 208 biological pathways in the following categories of the KEGG Pathway database (Table S9): Metabolism (except for global and overview maps), Environmental Information Processing (except for membrane transport and signaling molecules and interaction), Cellular Processes (except for transport and catabolism), and Organismal Systems.[7] A hypergeometric test was performed to estimate statistical significance, and all p-values for biological pathways of each drug and tumor type were adjusted by the Benjamini-Hochberg approach (adjusted p-values). The drug/cancer−pathway associations detected with adjusted p-values < 0.01 were considered more significant. For no associations between drugs/cancers and pathways, these drugs/cancers or pathways were removed from the networks.

3. RESULTS

3.1. Statistics of the Benchmark Data Sets. In this study, we used the drug-induced transcriptomics data from the L1000FWD data set and Affymetrix-based CMap data set to build the drug−pathway networks. There were eight drug−pathway networks and two external validation sets used to build and evaluate the models. The numbers of drugs, pathways, and associations for these drug−pathway networks are provided in Table 1.

Here, we focused on the pan-cancer network due to comprehensive drug−pathway associations, which contained 45 645 drug−pathway associations connecting 3455 drugs and 148 pathways (Table S2). On this basis, 80% of drugs and their drug−pathway associations were divided into training and test sets, including 36 883 drug−pathway associations connecting 2764 drugs and 142 pathways. The remaining 20% of drugs and their drug−pathway associations were considered as external validation set 1, containing 8762 drug−pathway associations connecting 691 drugs and 139 pathways (Table S4). The external validation set 2 from the Affymetrix-based

https://doi.org/10.1021/acs.jcim.1c00009
J. Chem. Inf. Model. 2021, 61, 2475−2485

Table 1. Statistics of Drug−Pathway Networks[a]

network	N_{Drug}	$N_{Pathway}$	N_{DP}	sparsity (%)
pan-cancer	3455	148	45645	8.93
breast cancer	1127	134	5758	3.81
colorectal cancer	1092	117	3501	2.74
kidney cancer	933	128	3472	2.91
liver cancer	763	113	2446	2.84
lung cancer	1362	130	7698	4.35
prostate cancer	2050	136	9711	3.48
skin cancer	1096	124	4319	3.18
external validation set 1	691	139	8762	9.12
external validation set 2	34	44	185	12.37

[a] N_{Drug}: the number of drugs. $N_{Pathway}$: the number of pathways. N_{DP}: the number of drug−pathway associations. Sparsity: the radio of N_{DP} and the number of all possible drug−pathway associations.

CMap data set contained 185 drug−pathway associations connecting 34 drugs and 44 pathways (Table S4). These two external validation sets were used to evaluate the model generalization ability. Other drug−pathway networks were used to build different primary site-based models by the DPNetinfer method. Meanwhile, the drug−substructure linkages of each drug in drug−pathway networks were created as a substructure−drug network. Finally, different substructure−drug−pathway networks were constructed for prediction and validation by integrating substructure−drug networks and drug−pathway networks.

3.2. Description of DPNetinfer Method. Here, we introduced the DPNetinfer method for prediction of drug−pathway association, mainly including (i) performance evaluation of DPNetinfer with cross validation and (ii) evaluation of model generalization ability using two external validation sets.

3.2.1. Performance Evaluation of the DPNetinfer Method. In this study, 10-fold cross validation was used to optimize the best condition and evaluate the performance of the DPNetinfer method. Here, we gave priority to the pan-cancer network to build a model. First, in the case of parameters $k = 2$ and $\gamma = 0$, the relationships among α, β, FPs, and the average AUC value of these models were shown in Figure S1. The results showed that the model performance for different FPs reached the maximum when $\alpha = 0.1$ and $\beta = 0.1$. This indicated that higher model performance should be tended to allocate initial resource to pathway nodes rather than substructure nodes and set bigger weighted values of drug−pathway associations than drug-substructure linkages. Subsequently, under the condition of $k = 2$, $\alpha = 0.1$, and $\beta = 0.1$, the optimal value of parameter γ was searched for each model. As shown in Figure 2, it revealed that the performance of most models could be maximized when $\gamma = -0.8$, and the influence of hub nodes could be weakened by setting a negative value of γ. In these models, the Morgan (1, 1024) FP had performed the best with the highest AUC value (0.9358 ± 0.0015). Following the same process as above, we also compared the effects of different resource diffusion numbers ($k = 2, 4, 6, 8, 10$) on the model performance under different FPs (Figure 3). The results

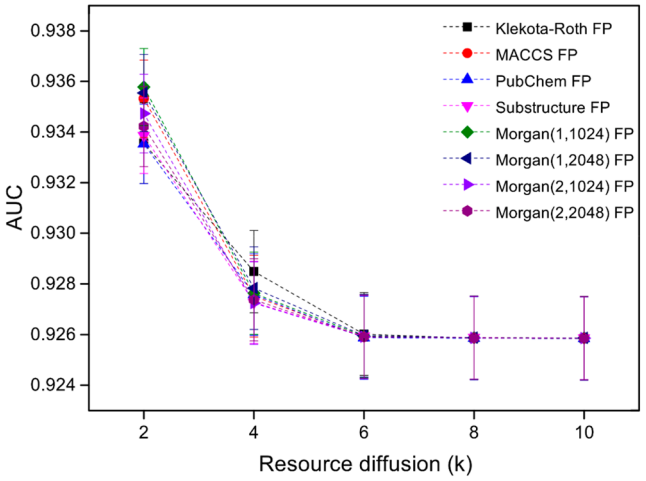

Figure 3. Relationships among parameter k, FPs, and the AUC value for the DPNetinfer method in 10-fold cross validation.

illustrated that no matter what type of FPs, the performance of models had always been the best when $k = 2$ and gradually decreased as the increase of k. The other evaluation indicators (P and R) of models also showed the same trend (Table S10). Even if there was not much difference among the optimal models of each molecular fingerprint under different parameter k. This just showed that the network-based method has good robustness. As a result, the DPNetinfer method performed well in a pan-cancer network under those conditions: $k = 2$, $\alpha = 0.1$, $\beta = 0.1$, $\gamma = -0.8$, and Morgan (1, 1024) FP.

3.2.2. Evaluation of Model Generalization Ability. Here, two external validation sets were used to evaluate the model

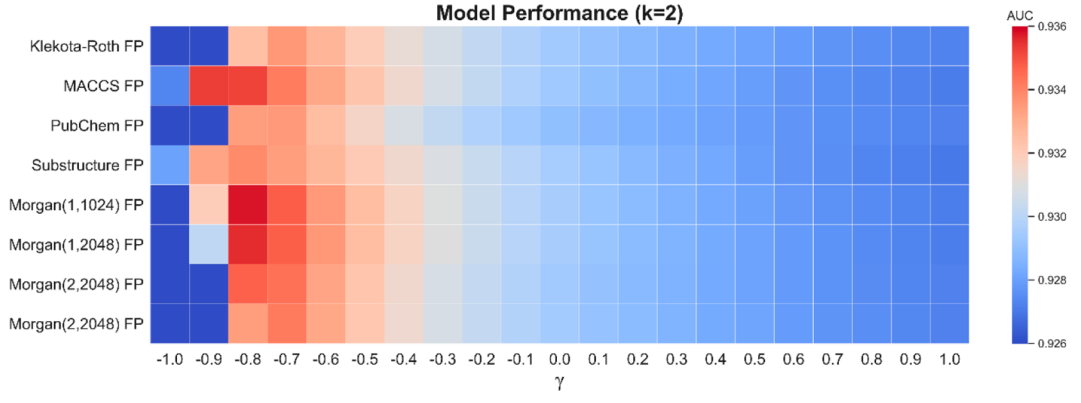

Figure 2. Relationships among parameter γ, FPs, and the average AUC value for the DPNetinfer method in 10-fold cross validation when $k = 2$. Setting AUC ≤ 0.926 to blue, and AUC ≥ 0.936 to red.

https://doi.org/10.1021/acs.jcim.1c00009
J. Chem. Inf. Model. 2021, 61, 2475−2485

generalization ability of DPNetinfer. As shown in Table 2, under the condition of $k = 2$ and Morgan (1, 1024) FP, the DPNetinfer method had the generalization ability on two external validation sets (AUC = 0.8519 and 0.7494), respectively. It was remarkable that the highest AUC values, 0.8710 and 0.7838, were yielded for DPNetinfer with PubChem FP, respectively. The possible reason might be that the sparsity of the external validation sets was relatively large (Table 1). Nevertheless, DPNetinfer was shown to have a good capability of generalization on two external validation sets.

Table 2. Model Generalization Ability of DPNetinfer in External Validation Sets When $k = 2$

data set	FP type	α	β	γ	AUC
external validation set 1	Klekota-Roth	0.1	0.1	−0.7	0.8662
	MACCS	0.1	0.1	−0.9	0.8500
	PubChem	0.1	0.1	−0.7	0.8710
	Substructure	0.1	0.1	−0.8	0.8542
	Morgan (1, 1024)	0.1	0.1	−0.8	0.8519
	Morgan (1, 2048)	0.1	0.1	−0.8	0.8497
	Morgan (2, 1024)	0.1	0.1	−0.8	0.8580
	Morgan (2, 2048)	0.1	0.1	−0.7	0.8518
external validation set 2	Klekota-Roth	0.1	0.1	−0.7	0.7828
	MACCS	0.1	0.1	−0.9	0.7527
	PubChem	0.1	0.1	−0.7	0.7838
	Substructure	0.1	0.1	−0.8	0.7599
	Morgan (1, 1024)	0.1	0.1	−0.8	0.7494
	Morgan (1, 2048)	0.1	0.1	−0.8	0.7489
	Morgan (2, 1024)	0.1	0.1	−0.8	0.7613
	Morgan (2, 2048)	0.1	0.1	−0.7	0.7525

3.2.3. Primary Site-Based DPNetinfer. According to primary sites of different tumor types, seven primary site-based models were built to predict drug−pathway associations using the DPNetinfer method. Each model was identified as the optimal model by 10-fold cross validation (Tables 3 and S11). In these models, the prostate cancer model performed well with AUC value at 0.9197 ± 0.0036, followed by the lung cancer model (0.9130 ± 0.0044), and the breast cancer model (0.9120 ± 0.0055). Thus, this way would be more conductive to discover specific and effective drug−pathway associations for different primary sites and avoid the problem of tumor heterogeneity.

Table 3. Performance of Primary Site-Based Models by DPNetinfer[a]

primary site	AUC	P ($L = 5$)	R ($L = 5$)
breast cancer	0.9120 ± 0.0055	0.1511 ± 0.0069	0.4785 ± 0.0253
colorectal cancer	0.9058 ± 0.0076	0.1291 ± 0.0074	0.5219 ± 0.0292
kidney cancer	0.8925 ± 0.0076	0.1133 ± 0.0074	0.4265 ± 0.0262
liver cancer	0.9013 ± 0.0085	0.1184 ± 0.0087	0.4714 ± 0.0328
lung cancer	0.9130 ± 0.0044	0.1470 ± 0.0054	0.4816 ± 0.0198
prostate cancer	0.9197 ± 0.0036	0.1406 ± 0.0044	0.5095 ± 0.0157
skin cancer	0.9019 ± 0.0060	0.1229 ± 0.0060	0.4653 ± 0.0235

[a]AUC: the areas under a receiver operating characteristic curve. P: precision. R: recall. L: the predicted drug−pathway associations in the top-length places for each drugs.

3.3. Case Study: Pathway-Based Drug Repurposing for Cancer Therapy. In the above work, we presented the DPNetinfer method to predict potential drug−pathway associations for old drugs, clinically failed drugs, and NCEs. As a case study, here we tried to discover the anticancer potentials of NCEs and nononcology drugs with the DPNetinfer method.

3.3.1. Pathway−Cancer Network. In this study, the pathway−cancer network (as shown in Figure 4) was constructed to analyze the critical role of pathways in cancer, which contained: 289 pathway−cancer associations connecting 21 tumor types and 110 pathways. For example, lung cancer (LUAD and LUSC) was mainly related to cell cycle (hsa04110). Breast cancer (BRCA) was mainly related to the PI3K-Akt pathway (hsa04151), MAPK pathway (hsa04010), and so on. Through network analysis, some pathways had a higher degree in the pathway−cancer network, such as focal adhesion (hsa04510, degree = 14), cell cycle (degree = 12), and PI3K-Akt pathway (degree = 10) (Figure S2). The results demonstrated that 80% of tumor types had at least one driver alteration for cell cycle pathway and PI3K-Akt pathway. Therefore, these cancer-related pathways provided useful information for pathway-based drug discovery, especially the PI3K-Akt pathway.

3.3.2. PI3K-Akt Pathway As Characterization of Anticancer Drugs. The anticancer activity data (IC_{50} on A549 cell line) of 46 NCEs were collected from the *Journal of Medicinal Chemistry* to identify PI3K-Akt pathway as characterization of anticancer drugs. Potential pathways of NCEs ($L \leq 6$) were predicted by the DPNetinfer method. As shown in Figure 5, the results showed that the IC_{50} values of NCEs linked to the PI3K-Akt pathway were lower than those of NCEs not linked to the PI3K-Akt pathway (Wilcoxon test: p-value = 0.0013). Other pathways did not show significant differences. In other words, drugs linked to the PI3K-Akt pathway had the potential to be anticancer drugs. Meanwhile, the Pearson correlation analysis was used to analyze the correlation between PI3K-Akt pathway and the IC_{50} value ($r = -0.6489$, p-value = 1.08×10^{-6}), which further illustrated that drugs linked to the PI3K-Akt pathway could have powerful anticancer efficacy. Furthermore, these potential associations between PI3K-Akt pathway and approved anticancer drugs from DrugBank database were predicted by the DPNetinfer method under different L values (Table S8). With the increase of L, the recall rate of anticancer drugs had been increased (Figure S3), but the precision rate could be reduced (due to the negative correlation between the recall rate and the precision rate). For this reason, $L \leq 6$ was recommended to ensure the performance of DPNetinfer and the top ranked drug−pathway associations were given the priority. In addition, among 24 anticancer drugs from CCLE database (Table S7), 19 ones had potential associations with the PI3K-Akt pathway ($L \leq 6$). As a result, the PI3K-Akt pathway would be given priority to the characterization of anticancer drugs.

3.3.3. Anticancer Potential of Nononcology Drugs. To evaluate the predictive capability of pathway-based drug

https://doi.org/10.1021/acs.jcim.1c00009
J. Chem. Inf. Model. 2021, 61, 2475−2485

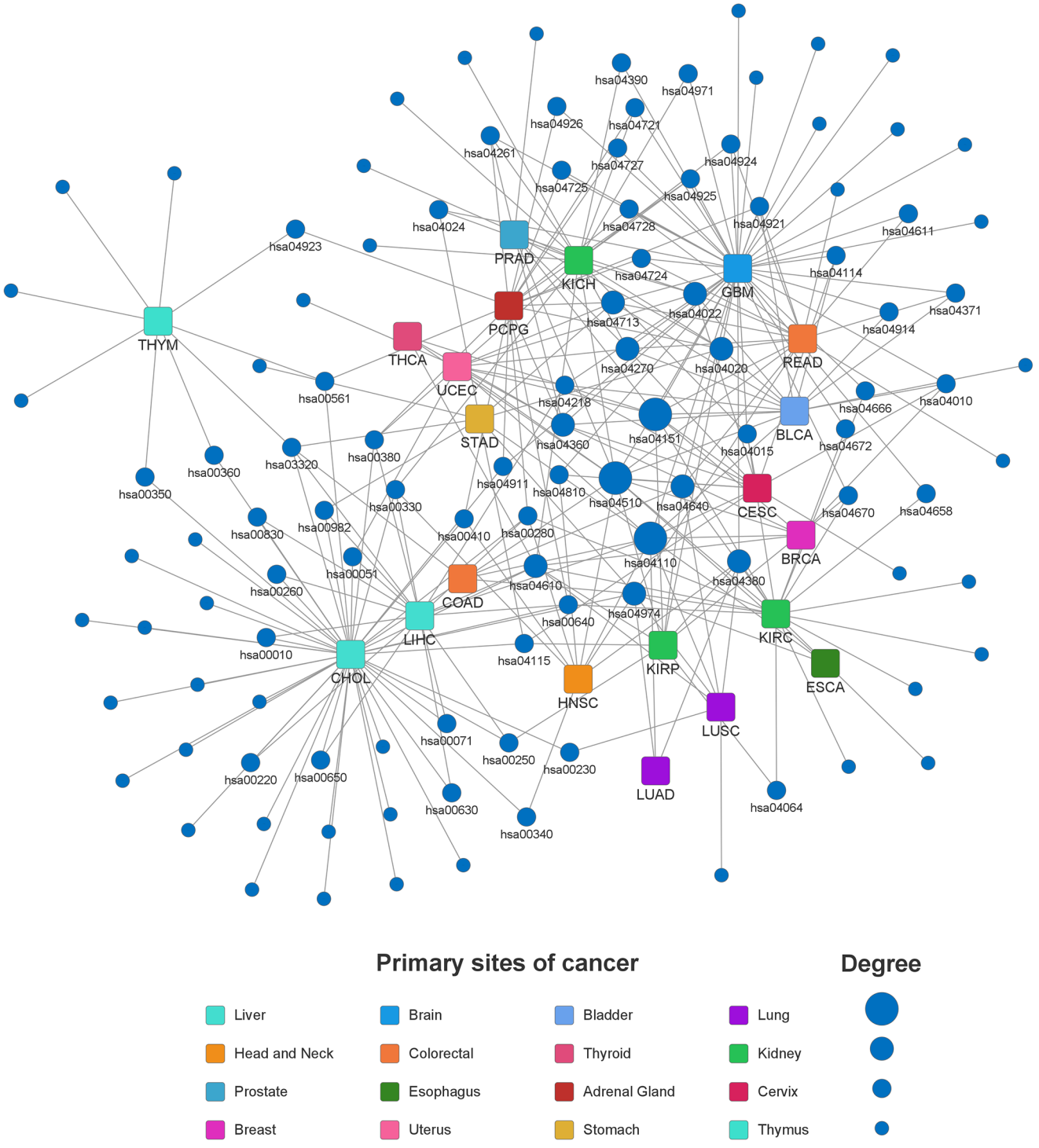

Figure 4. Pathway−cancer network. The rectangles of different colors represent primary sites of different cancer types. The blue circular nodes represent pathways, and their size indicates the values of degree in the network.

repurposing with DPNetinfer, we performed a large-scale prediction of potential anticancer effects for approved nononcology drugs from the DrugBank database. Here we only focused on the top ranked drug−pathway associations ($L \leq 3$). By predicting potential drug−pathway associations for 1293 nononcology drugs, 66 nononcology drugs had potential associations with the PI3K-Akt pathway (Table S8). Subsequently, about 24% nononcology drugs (16/66) had been identified the anticancer potential by literature (Table 4) and the PRISM drug repurposing source[37] (Table S12). For instance, statins and antidiabetic drugs inhibited cancer cell proliferation. The anticancer activity (IC_{50}) of lovastatin was 6−8 μM in lung cancer cell lines. The anticancer activity (IC_{50}) of cyproterone acetate was 3−4 μM in colorectal and lung cancer cell lines. The anticancer activity (IC_{50}) of fluorometholone was 0.5−1 μM in different cancer cell lines. For other nononcology drugs, their potential anticancer efficacies need further experimental verification. Taken

https://doi.org/10.1021/acs.jcim.1c00009
J. Chem. Inf. Model. 2021, 61, 2475−2485

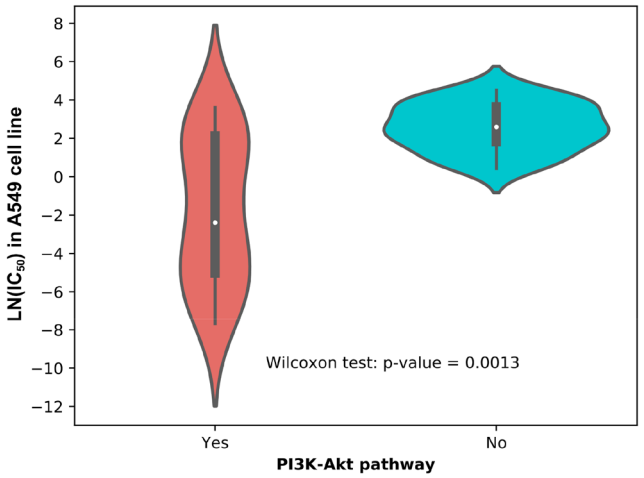

Figure 5. PI3K-Akt pathway as a characterization of anticancer drugs by the Wilcoxon rank sum test. LN is the log base e (natural logarithm). "Yes" represents the associations between drugs and the PI3K-Akt pathway. "No" represents no association between drugs and the PI3K-Akt pathway.

together, DPNetinfer offered a powerful tool to identify the unexpected anticancer activity of some nononcology drugs by the PI3K-Akt pathway.

4. DISCUSSION

4.1. DPNetinfer is a Powerful Tool for Prediction of Drug−Pathway Associations. In this study, we introduced a novel computational method for prediction of drug−pathway associations named DPNetinfer, which was constructed by integrating substructure−drug−pathway network with bSDTNBI method. Based on systematic evaluation, the DPNetinfer method performed well in the pan-cancer network under the conditions: $k = 2$, $\alpha = 0.1$, $\beta = 0.1$, $\gamma = -0.8$, and Morgan (1, 1024) FP. Furthermore, it showed good model generalization capability on external validation sets. Compared with previously published methods,[7,13,14] the novelty of our method showed such advantages as independence of negative samples and using chemical substructures as the bridge of drugs and pathways to predict drug−pathway associations for old drugs, clinically failed drugs, and NCEs.

The drug−pathway network from drug-induced transcriptomics data provided a global view of intracellular pathways under the perturbation of drugs. Meanwhile, pathway-based characterization was screened according to KEGG categories in this work, which would pay more attentions to the changes of intracellular functions under different treatments. Although some databases provided drug−pathway data sets based on target-association and gene-association such as TTD[57] and CTD databases,[58] it could not be truly mapped to a global view of intracellular pathways under the perturbation of drugs. Some existing methods[16,59,60] do not provide training data, user interfaces, or tools; it is difficult to repeat those works. This leads to the fact that our proposed method cannot be compared with others directly. In order to make up for the shortcoming, the DPNetinfer method was evaluated by external validation sets from different drug-induced transcriptomics data and achieved good capability of generalization. Thus, the DPNetinfer method would provide a powerful tool for prediction of drug−pathway associations.

4.2. Pathway-Based Drug Repurposing for Cancer Therapy. As a case study, DPNetinfer was used in pathway-based drug repurposing for cancer therapy. From the perspective of network medicine, drugs sharing similar therapeutic functions may be involved in similar pathways associated with certain pathological process.[2] In this work, we assumed that if drugs acted on the same cancer-related pathways, these drugs would share similar therapeutic functions and be potential anticancer drugs. Through the collection and analysis of anticancer activity data and known anticancer drugs, the PI3K-Akt pathway was regarded as priority of anticancer drugs. Previous studies confirmed that the PI3K-Akt pathway is closely related to tumorigenesis and development.[5]

Subsequently, the unexpected anticancer activities of some nononcology drugs were predicted by the DPNetinfer method (Tables 4 and S12) and confirmed by newly experimental evidence. For instance, pravastatin could inhibit cell proliferation by increasing MAT1A expression in cancer cell lines,[38,39] while simvastatin was found to suppress breast cancer with tumor vascular normalization.[40,41] Sitagliptin would affect gastric cancer cells proliferation by suppressing melanoma-associated antigen-A3 expression.[42] In another network-based drug repurposing approach we developed for prediction of ATC codes,[24] a very good consistency (62% coverage with $L \leq 3$) was obtained with this DPNetinfer method (Table S8).

Table 4. Anticancer Potential of Nononcology Drugs Linked to the PI3K-Akt Pathway ($L = 3$) Based on the DPNetinfer Method

DrugBank ID	drug name	original indication	drug repurposing
DB00175	pravastatin	hypercholesterolemia	hepatocellular carcinoma[38,39]
DB00641	simvastatin	hyperlipidemia	breast cancer[40,41]
DB01261	sitagliptin	type 2 diabetes mellitus	gastric cancer[42]
DB00357	aminoglutethimide	cushing's syndrome	breast cancer[43]
DB00421	spironolactone	potassium sparing diuretic	prostate cancer[44]
DB00663	flumethasone	dermatitis	lung cancer[45]
DB01234	dexamethasone	autoimmune inflammatory diseases	breast and lung cancers[46]
DB00806	pentoxifylline	chronic occlusive arterial disease	pancreatic cancer[47,48]
DB00982	isotretinoin	nodular acne	renal cancer[49]
DB00284	acarbose	type 2 diabetes mellitus	breast and renal cancers[50,51]
DB00826	natamycin	antifungal agent	prostate cancer[52]
DB06697	artemether	malaria	breast and lung cancers[53,54]
DB09274	artesunate	malaria	bladder and breast cancers[55,56]

https://doi.org/10.1021/acs.jcim.1c00009
J. Chem. Inf. Model. 2021, 61, 2475−2485

Therefore, DPNetinfer would provide a new way to drug repurposing.

5. CONCLUSIONS

In this study, DPNetinfer was developed as an effective and low-cost tool for large-scale prediction of drug−pathway associations, and it was demonstrated to have good predictive accuracy in pathway-based drug repurposing for cancer therapy. Nevertheless, there is still a room for us to improve the DPNetinfer method. For example, it is difficult to pinpoint which protein (protein active site) in the pathway is responsible for the association, because the three-dimensional structures of most proteins in the human proteome have not be determined yet. The type of action (activation and inhibition) between drugs and pathways cannot be predicted. In the next step, these issues would be considered to improve the method.

DPNetinfer was deployed to the NetInfer web server (http://lmmd.ecust.edu.cn/netinfer/). With the web server,[61] users can easily predict drug−pathway associations by selecting the prediction type as "Pathways", in addition to the prediction of target proteins, microRNAs, ATC codes, and ADEs for drugs. We hope the web server would be helpful for drug discovery and development.

DATA AND SOFTWARE AVAILABILITY

All data involved in this study are available with the paper (see the Supporting Information). The software used to execute the study and prepare the figures in the manuscript are freely available as follows: Cytoscape (https://cytoscape.org/), PaDEL-Descriptor (http://padel.nus.edu.sg/software/padeldescriptor). The commercial software platform Pipeline Pilot was purchased by East China University of Science and Technology and licensed from BIOVIA (https://www.3ds.com/products-services/biovia/products/data-science/pipeline-pilot/).

ASSOCIATED CONTENT

Supporting Information

The Supporting Information is available free of charge at https://pubs.acs.org/doi/10.1021/acs.jcim.1c00009.

Figure S1: Relationships among parameters α, β, FPs, and the average AUC value for the DPNetinfer method in 10-fold cross validation when $k = 2$. Figure S2: Degree distribution of pathways in the pathway−cancer network. Figure S3: Recall rate of approved anticancer drugs from DrugBank database by the DPNetinfer method under different L values (PDF)

Table S1: Drug-induced transcriptome data from L1000FWD data set. Table S2: Drug−pathway associations of the pan-cancer network. Table S3: Drug-induced transcriptome data from Affymetrix-based CMap data set. Table S4: Drug−pathway network of external validation sets. Table S5: RNA-Seq (read counts) data of different tumor types. Table S6: IC_{50} activity data of NCEs in A549 cell line from references. Table S7: Known anticancer drugs from CCLE database. Table S8: Approved oncology and nononcology drugs from DrugBank database. Table S9: Biological pathways in the KEGG Pathway database. Table S10: Evaluation indicators (P and R) of the DPNetinfer method. Table S11: Optimal parameters and FPs of different primary-site models. Table S12: Anticancer activity (IC_{50}) of nononcology drugs linked to the PI3K-Akt pathway in the human cancer cell lines (XLSX)

AUTHOR INFORMATION

Corresponding Author

Yun Tang − *Shanghai Key Laboratory of New Drug Design, School of Pharmacy, East China University of Science and Technology, Shanghai 200237, China;* orcid.org/0000-0003-2340-1109; Email: ytang234@ecust.edu.cn

Authors

Jiye Wang − *Shanghai Key Laboratory of New Drug Design, School of Pharmacy, East China University of Science and Technology, Shanghai 200237, China;* orcid.org/0000-0002-5568-1515

Zengrui Wu − *Shanghai Key Laboratory of New Drug Design, School of Pharmacy, East China University of Science and Technology, Shanghai 200237, China;* orcid.org/0000-0003-3095-6006

Yayuan Peng − *Shanghai Key Laboratory of New Drug Design, School of Pharmacy, East China University of Science and Technology, Shanghai 200237, China;* orcid.org/0000-0003-2669-9684

Weihua Li − *Shanghai Key Laboratory of New Drug Design, School of Pharmacy, East China University of Science and Technology, Shanghai 200237, China;* orcid.org/0000-0001-7055-9836

Guixia Liu − *Shanghai Key Laboratory of New Drug Design, School of Pharmacy, East China University of Science and Technology, Shanghai 200237, China;* orcid.org/0000-0001-9648-844X

Complete contact information is available at: https://pubs.acs.org/10.1021/acs.jcim.1c00009

Author Contributions

#J.W. and Z.W. contributed equally to this work. Y.T. conceived and directed the project. J.W., Z.W., and Y.T. designed the study. J.W. collected the benchmark data sets and carried out the experiments. Z.W. deployed the DPNetinfer method to the NetInfer Web site. J.W., Y.P., W.L., and G.L. performed the analysis. J.W., Z.W., and Y.T. interpreted the results and wrote the manuscript. All authors read and approved the final manuscript.

Notes

The authors declare no competing financial interest.

ACKNOWLEDGMENTS

This work was supported by the National Key Research and Development Program of China (grants 2016YFA0502304 and 2019YFA0904800), the National Natural Science Foundation of China (grants 81673356 and 81872800), the China Postdoctoral Science Foundation (grant 2019M661413), and Shanghai Sailing Program (grant 19YF1412700).

REFERENCES

(1) Hopkins, A. L. Network pharmacology: the next paradigm in drug discovery. *Nat. Chem. Biol.* **2008**, *4*, 682−90.

(2) Barabási, A. L.; Gulbahce, N.; Loscalzo, J. Network medicine: a network-based approach to human disease. *Nat. Rev. Genet.* **2011**, *12*, 56−68.

(3) Cheng, F.; Lu, W.; Liu, C.; Fang, J.; Hou, Y.; Handy, D. E.; Wang, R.; Zhao, Y.; Yang, Y.; Huang, J.; Hill, D. E.; Vidal, M.; Eng,

C.; Loscalzo, J. A genome-wide positioning systems network algorithm for in silico drug repurposing. *Nat. Commun.* **2019**, *10*, 3476.
(4) Wilhelm, S. M.; Carter, C.; Tang, L.; Wilkie, D.; McNabola, A.; Rong, H.; Chen, C.; Zhang, X.; Vincent, P.; McHugh, M.; Cao, Y.; Shujath, J.; Gawlak, S.; Eveleigh, D.; Rowley, B.; Liu, L.; Adnane, L.; Lynch, M.; Auclair, D.; Taylor, I.; Gedrich, R.; Voznesensky, A.; Riedl, B.; Post, L. E.; Bollag, G.; Trail, P. A. BAY 43−9006 Exhibits Broad Spectrum Oral Antitumor Activity and Targets the RAF/MEK/ERK Pathway and Receptor Tyrosine Kinases Involved in Tumor Progression and Angiogenesis. *Cancer Res.* **2004**, *64*, 7099−7109.
(5) Vogelstein, B.; Kinzler, K. W. Cancer genes and the pathways they control. *Nat. Med.* **2004**, *10*, 789−799.
(6) Li, J. J. *Medicinal Chemistry for Practitioners*; John Wiley & Sons, 2020.
(7) Iwata, M.; Hirose, L.; Kohara, H.; Liao, J.; Sawada, R.; Akiyoshi, S.; Tani, K.; Yamanishi, Y. Pathway-Based Drug Repositioning for Cancers: Computational Prediction and Experimental Validation. *J. Med. Chem.* **2018**, *61*, 9583−9595.
(8) Pushpakom, S.; Iorio, F.; Eyers, P. A.; Escott, K. J.; Hopper, S.; Wells, A.; Doig, A.; Guilliams, T.; Latimer, J.; McNamee, C.; Norris, A.; Sanseau, P.; Cavalla, D.; Pirmohamed, M. Drug repurposing: progress, challenges and recommendations. *Nat. Rev. Drug Discovery* **2019**, *18*, 41−58.
(9) Wang, C. C.; Zhao, Y.; Chen, X. Drug-pathway association prediction: from experimental results to computational models. *Briefings Bioinf.* **2020**, DOI: 10.1093/bib/bbaa061.
(10) Hansen, J.; Galatioto, J.; Caescu, C. I.; Arnaud, P.; Calizo, R. C.; Spronck, B.; Murtada, S.-I.; Borkar, R.; Weinberg, A.; Azeloglu, E. U.; Bintanel-Morcillo, M.; Gallo, J. M.; Humphrey, J. D.; Jondeau, G.; Boileau, C.; Ramirez, F.; Iyengar, R. Systems pharmacology-based integration of human and mouse data for drug repurposing to treat thoracic aneurysms. *JCI Insight.* **2019**, *4*, No. e127652.
(11) Noh, H.; Shoemaker, J. E.; Gunawan, R. Network perturbation analysis of gene transcriptional profiles reveals protein targets and mechanism of action of drugs and influenza A viral infection. *Nucleic Acids Res.* **2018**, *46*, No. e34.
(12) Subramanian, A.; Narayan, R.; Corsello, S. M.; Peck, D. D.; Natoli, T. E.; Lu, X.; Gould, J.; Davis, J. F.; Tubelli, A. A.; Asiedu, J. K.; Lahr, D. L.; Hirschman, J. E.; Liu, Z.; Donahue, M.; Julian, B.; Khan, M.; Wadden, D.; Smith, I. C.; Lam, D.; Liberzon, A.; Toder, C.; Bagul, M.; Orzechowski, M.; Enache, O. M.; Piccioni, F.; Johnson, S. A.; Lyons, N. J.; Berger, A. H.; Shamji, A. F.; Brooks, A. N.; Vrcic, A.; Flynn, C.; Rosains, J.; Takeda, D. Y.; Hu, R.; Davison, D.; Lamb, J.; Ardlie, K.; Hogstrom, L.; Greenside, P.; Gray, N. S.; Clemons, P. A.; Silver, S.; Wu, X.; Zhao, W. N.; Read-Button, W.; Wu, X.; Haggarty, S. J.; Ronco, L. V.; Boehm, J. S.; Schreiber, S. L.; Doench, J. G.; Bittker, J. A.; Root, D. E.; Wong, B.; Golub, T. R. A Next Generation Connectivity Map: L1000 Platform and the First 1,000,000 Profiles. *Cell* **2017**, *171*, 1437−1452.
(13) Ma, H.; Zhao, H. iFad: an integrative factor analysis model for drug−pathway association inference. *Bioinformatics* **2012**, *28*, 1911−1918.
(14) Ma, H.; Zhao, H. FacPad: Bayesian sparse factor modeling for the inference of pathways responsive to drug treatment. *Bioinformatics* **2012**, *28*, 2662−2670.
(15) Li, C.; Yang, C.; Hather, G.; Liu, R.; Zhao, H. Efficient Drug-Pathway Association Analysis via Integrative Penalized Matrix Decomposition. *IEEE/ACM Trans. Comput. Biol. Bioinf.* **2016**, *13*, 531−40.
(16) Song, M.; Yan, Y.; Jiang, Z. Drug-pathway interaction prediction via multiple feature fusion. *Mol. BioSyst.* **2014**, *10*, 2907−2913.
(17) Napolitano, F.; Carrella, D.; Mandriani, B.; Pisonero-Vaquero, S.; Sirci, F.; Medina, D. L.; Brunetti-Pierri, N.; di Bernardo, D. gene2drug: a computational tool for pathway-based rational drug repositioning. *Bioinformatics* **2018**, *34*, 1498−1505.
(18) Mejia-Pedroza, R. A.; Espinal-Enriquez, J.; Hernandez-Lemus, E. Pathway-Based Drug Repositioning for Breast Cancer Molecular Subtypes. *Front. Pharmacol.* **2018**, *9*, 905.
(19) Li, J.; Lu, Z. Pathway-based drug repositioning using causal inference. *BMC Bioinf.* **2013**, *14*, S3.
(20) Cheng, F.; Liu, C.; Jiang, J.; Lu, W.; Li, W.; Liu, G.; Zhou, W.; Huang, J.; Tang, Y. Prediction of drug-target interactions and drug repositioning via network-based inference. *PLoS Comput. Biol.* **2012**, *8*, No. e1002503.
(21) Wu, Z.; Cheng, F.; Li, J.; Li, W.; Liu, G.; Tang, Y. SDTNBI: an integrated network and chemoinformatics tool for systematic prediction of drug-target interactions and drug repositioning. *Briefings Bioinf.* **2016**, *18*, 333−347.
(22) Wu, Z.; Lu, W.; Wu, D.; Luo, A.; Bian, H.; Li, J.; Li, W.; Liu, G.; Huang, J.; Cheng, F.; Tang, Y. In silico prediction of chemical mechanism of action via an improved network-based inference method. *Br. J. Pharmacol.* **2016**, *173*, 3372−3385.
(23) Li, J.; Lei, K.; Wu, Z.; Li, W.; Liu, G.; Liu, J.; Cheng, F.; Tang, Y. Network-based identification of microRNAs as potential pharmacogenomic biomarkers for anticancer drugs. *Oncotarget.* **2016**, *7*, 45584−45596.
(24) Peng, Y.; Wang, M.; Xu, Y.; Wu, Z.; Wang, J.; Zhang, C.; Liu, G.; Li, W.; Li, J.; Tang, Y. Drug repositioning by prediction of drug's anatomical therapeutic chemical code via network-based inference approaches. *Briefings Bioinf.* **2021**, *22*, 2058.
(25) Cheng, F.; Li, W.; Wang, X.; Zhou, Y.; Wu, Z.; Shen, J.; Tang, Y. Adverse Drug Events: Database Construction and in Silico Prediction. *J. Chem. Inf. Model.* **2013**, *53*, 744−752.
(26) Wang, Z.; Lachmann, A.; Keenan, A. B.; Ma'ayan, A. L1000FWD: fireworks visualization of drug-induced transcriptomic signatures. *Bioinformatics* **2018**, *34*, 2150−2152.
(27) Yap, C. W. PaDEL-descriptor: An open source software to calculate molecular descriptors and fingerprints. *J. Comput. Chem.* **2011**, *32*, 1466−1474.
(28) Lü, L.; Medo, M.; Yeung, C. H.; Zhang, Y.-C.; Zhang, Z.-K.; Zhou, T. Recommender systems. *Phys. Rep.* **2012**, *519*, 1−49.
(29) Love, M. I.; Huber, W.; Anders, S. Moderated estimation of fold change and dispersion for RNA-seq data with DESeq2. *Genome Biol.* **2014**, *15*, 550.
(30) Assenov, Y.; Ramírez, F.; Schelhorn, S.-E.; Lengauer, T.; Albrecht, M. Computing topological parameters of biological networks. *Bioinformatics* **2008**, *24*, 282−284.
(31) Kwon, Y.; Song, J.; Lee, H.; Kim, E. Y.; Lee, K.; Lee, S. K.; Kim, S. Design, Synthesis, and Biological Activity of Sulfonamide Analogues of Antofine and Cryptopleurine as Potent and Orally Active Antitumor Agents. *J. Med. Chem.* **2015**, *58*, 7749−62.
(32) Zhang, X. R.; Wang, H. W.; Tang, W. L.; Zhang, Y.; Yang, H.; Hu, D. X.; Ravji, A.; Marchand, C.; Kiselev, E.; Ofori-Atta, K.; Agama, K.; Pommier, Y.; An, L. K. Discovery, Synthesis, and Evaluation of Oxynitidine Derivatives as Dual Inhibitors of DNA Topoisomerase IB (TOP1) and Tyrosyl-DNA Phosphodiesterase 1 (TDP1), and Potential Antitumor Agents. *J. Med. Chem.* **2018**, *61*, 9908−9930.
(33) Liu, Z.; Wang, M.; Wang, H.; Fang, L.; Gou, S. Platinum-Based Modification of Styrylbenzylsulfones as Multifunctional Antitumor Agents: Targeting the RAS/RAF Pathway, Enhancing Antitumor Activity, and Overcoming Multidrug Resistance. *J. Med. Chem.* **2020**, *63*, 186−204.
(34) Barretina, J.; Caponigro, G.; Stransky, N.; Venkatesan, K.; Margolin, A. A.; Kim, S.; Wilson, C. J.; Lehár, J.; Kryukov, G. V.; Sonkin, D.; Reddy, A.; Liu, M.; Murray, L.; Berger, M. F.; Monahan, J. E.; Morais, P.; Meltzer, J.; Korejwa, A.; Jané-Valbuena, J.; Mapa, F. A.; Thibault, J.; Bric-Furlong, E.; Raman, P.; Shipway, A.; Engels, I. H.; Cheng, J.; Yu, G. K.; Yu, J.; Aspesi, P.; de Silva, M.; Jagtap, K.; Jones, M. D.; Wang, L.; Hatton, C.; Palescandolo, E.; Gupta, S.; Mahan, S.; Sougnez, C.; Onofrio, R. C.; Liefeld, T.; MacConaill, L.; Winckler, W.; Reich, M.; Li, N.; Mesirov, J. P.; Gabriel, S. B.; Getz, G.; Ardlie, K.; Chan, V.; Myer, V. E.; Weber, B. L.; Porter, J.; Warmuth, M.; Finan, P.; Harris, J. L.; Meyerson, M.; Golub, T. R.; Morrissey, M. P.; Sellers, W. R.; Schlegel, R.; Garraway, L. A. The Cancer Cell Line

Encyclopedia enables predictive modelling of anticancer drug sensitivity. *Nature* **2012**, *483*, 603−607.
(35) Wishart, D. S.; Feunang, Y. D.; Guo, A. C.; Lo, E. J.; Marcu, A.; Grant, J. R.; Sajed, T.; Johnson, D.; Li, C.; Sayeeda, Z.; Assempour, N.; Iynkkaran, I.; Liu, Y.; Maciejewski, A.; Gale, N.; Wilson, A.; Chin, L.; Cummings, R.; Le, D.; Pon, A.; Knox, C.; Wilson, M. DrugBank 5.0: a major update to the DrugBank database for 2018. *Nucleic Acids Res.* **2018**, *46*, D1074−D1082.
(36) Yu, G.; Wang, L.-G.; Han, Y.; He, Q.-Y. clusterProfiler: an R Package for Comparing Biological Themes Among Gene Clusters. *OMICS* **2012**, *16*, 284−287.
(37) Corsello, S. M.; Nagari, R. T.; Spangler, R. D.; Rossen, J.; Kocak, M.; Bryan, J. G.; Humeidi, R.; Peck, D.; Wu, X.; Tang, A. A.; Wang, V. M.; Bender, S. A.; Lemire, E.; Narayan, R.; Montgomery, P.; Ben-David, U.; Garvie, C. W.; Chen, Y.; Rees, M. G.; Lyons, N. J.; McFarland, J. M.; Wong, B. T.; Wang, L.; Dumont, N.; O'Hearn, P. J.; Stefan, E.; Doench, J. G.; Harrington, C. N.; Greulich, H.; Meyerson, M.; Vazquez, F.; Subramanian, A.; Roth, J. A.; Bittker, J. A.; Boehm, J. S.; Mader, C. C.; Tsherniak, A.; Golub, T. R. Discovering the anti-cancer potential of non-oncology drugs by systematic viability profiling. *Nat. Cancer.* **2020**, *1*, 235−248.
(38) Riaño, I.; Martín, L.; Varela, M.; Serrano, T.; Núñez, O.; Mínguez, B.; Rodrigues, P. M.; Perugorria, M. J.; Banales, J. M.; Arenas, J. I. Efficacy and Safety of the Combination of Pravastatin and Sorafenib for the Treatment of Advanced Hepatocellular Carcinoma (ESTAHEP Clinical Trial). *Cancers* **2020**, *12*, 1900.
(39) Hijona, E.; Banales, J. M.; Hijona, L.; Medina, J. F.; Arenas, J.; Herreros-Villanueva, M.; Aldazabal, P.; Bujanda, L. Pravastatin inhibits cell proliferation and increased MAT1A expression in hepatocarcinoma cells and in vivo models. *Cancer Cell Int.* **2012**, *12*, 5.
(40) Yuan, W.; Hai, B.; Ren, X.; Zhu, J.; Zhang, C.; Guan, Z.; Jia, J.; Wang, H.; Cao, B.; Song, C. Single-dose local intraosseous injection of simvastatin suppresses breast cancer with tumor vascular normalization. *Transl. Oncol.* **2020**, *13*, 100867.
(41) Chen, C.; Wu, H.; Kong, D.; Xu, Y.; Zhang, Z.; Chen, F.; Zou, L.; Li, Z.; Shui, J.; Luo, H.; Liu, S.-H.; Yu, J.; Wang, K.; Brunicardi, F. C. Transcriptome sequencing analysis reveals unique and shared antitumor effects of three statins in pancreatic cancer. *Oncol. Rep.* **2020**, *44*, 2569−2580.
(42) Wang, Q.; Lu, P.; Wang, T.; Zheng, Q.; Li, Y.; Leng, S. X.; Meng, X.; Wang, B.; Xie, J.; Zhang, H. Sitagliptin affects gastric cancer cells proliferation by suppressing Melanoma-associated antigen-A3 expression through Yes-associated protein inactivation. *Cancer Med.* **2020**, *9*, 3816−3828.
(43) Geisler, J.; Johannessen, D. C.; Anker, G.; Lønning, P. E. Treatment with formestane alone and in combination with amino-glutethimide in heavily pretreated breast cancer patients: Clinical and endocrine effects. *Eur. J. Cancer* **1996**, *32*, 789−792.
(44) Hiebert, B. M.; Janzen, B. W.; Sanjanwala, R. M.; Ong, A. D.; Feldman, R. D.; Kim, J. O. Impact of Spironolactone Exposure on Prostate Cancer Incidence Amongst Men with Heart Failure: A Pharmacoepidemiologic Study. *Br. J. Clin. Pharmacol.* **2021**, *87*, 1801.
(45) Zhou, Y.; Zhou, Y.; Wang, K.; Li, T.; Yang, M.; Wang, R.; Chen, Y.; Cao, M.; Hu, R. Flumethasone enhances the efficacy of chemotherapeutic drugs in lung cancer by inhibiting Nrf2 signaling pathway. *Cancer Lett.* **2020**, *474*, 94−105.
(46) Jeon, M. Y.; Woo, S. M.; Seo, S. U.; Kim, S. H.; Nam, J.-O.; Kim, S.; Park, J.-W.; Kubatka, P.; Min, K.-J.; Kwon, T. K. Dexamethasone Inhibits TRAIL-Induced Apoptosis through c-FLIP-(L) Upregulation and DR5 Downregulation by GSK3β Activation in Cancer Cells. *Cancers* **2020**, *12*, 2901.
(47) Nandi, T.; Pradyuth, S.; Singh, A. K.; Chitkara, D.; Mittal, A. Therapeutic agents for targeting desmoplasia: current status and emerging trends. *Drug Discovery Today* **2020**, *25*, 2046.
(48) Kim, J. H.; Shin, B. C.; Park, W. S.; Lee, J.; Kuh, H. J. Antifibrotic effects of pentoxifylline improve the efficacy of gemcitabine in human pancreatic tumor xenografts. *Cancer Sci.* **2017**, *108*, 2470−2477.
(49) Molina, A. M.; van der Mijn, J. C.; Christos, P.; Wright, J.; Thomas, C.; Dutcher, J. P.; Nanus, D. M.; Tagawa, S. T.; Gudas, L. J. NCI 6896: a phase I trial of vorinostat (SAHA) and isotretinoin (13-cis retinoic acid) in the treatment of patients with advanced renal cell carcinoma. *Invest. New Drugs* **2020**, *38*, 1383−1389.
(50) Orlandella, R. M.; Turbitt, W. J.; Gibson, J. T.; Boi, S. K.; Li, P.; Smith, D. L., Jr.; Norian, L. A. The Antidiabetic Agent Acarbose Improves Anti-PD-1 and Rapamycin Efficacy in Preclinical Renal Cancer. *Cancers* **2020**, *12*, 2872.
(51) Zare, S.; Mirkhani, H.; Firuzi, O.; Moheimanian, N.; Asadollahi, M.; Pirhadi, S.; Chandran, J. N.; Schneider, B.; Jassbi, A. R. Antidiabetic and cytotoxic polyhydroxylated oleanane and ursane type triterpenoids from Salvia grossheimii. *Bioorg. Chem.* **2020**, *104*, 104297.
(52) Vasquez, J. L.; Lai, Y.; Annamalai, T.; Jiang, Z.; Zhang, M.; Lei, R.; Zhang, Z.; Liu, Y.; Tse-Dinh, Y.-C.; Agoulnik, I. U. Inhibition of base excision repair by natamycin suppresses prostate cancer cell proliferation. *Biochimie* **2020**, *168*, 241−250.
(53) Khatri, H.; Chokshi, N.; Rawal, S.; Patel, B. M.; Badanthadka, M.; Patel, M. M. Fabrication and in vivo evaluation of ligand appended paclitaxel and artemether loaded lipid nanoparticulate systems for the treatment of NSCLC: A nanoparticle assisted combination oncotherapy. *Int. J. Pharm.* **2020**, *583*, 119386.
(54) Akbarian, A.; Ebtekar, M.; Pakravan, N.; Hassan, Z. M. Folate receptor alpha targeted delivery of artemether to breast cancer cells with folate-decorated human serum albumin nanoparticles. *Int. J. Biol. Macromol.* **2020**, *152*, 90−101.
(55) Zhou, X.; Chen, Y.; Wang, F.; Wu, H.; Zhang, Y.; Liu, J.; Cai, Y.; Huang, S.; He, N.; Hu, Z.; Jin, X. Artesunate induces autophagy dependent apoptosis through upregulating ROS and activating AMPK-mTOR-ULK1 axis in human bladder cancer cells. *Chem.-Biol. Interact.* **2020**, *331*, 109273.
(56) Pirali, M.; Taheri, M.; Zarei, S.; Majidi, M.; Ghafouri, H. Artesunate, as a HSP70 ATPase activity inhibitor, induces apoptosis in breast cancer cells. *Int. J. Biol. Macromol.* **2020**, *164*, 3369−3375.
(57) Wang, Y.; Zhang, S.; Li, F.; Zhou, Y.; Zhang, Y.; Wang, Z.; Zhang, R.; Zhu, J.; Ren, Y.; Tan, Y.; Qin, C.; Li, Y.; Li, X.; Chen, Y.; Zhu, F. Therapeutic target database 2020: enriched resource for facilitating research and early development of targeted therapeutics. *Nucleic Acids Res.* **2019**, *48*, D1031−D1041.
(58) Davis, A. P.; Grondin, C. J.; Johnson, R. J.; Sciaky, D.; McMorran, R.; Wiegers, J.; Wiegers, T. C.; Mattingly, C. J. The Comparative Toxicogenomics Database: update 2019. *Nucleic Acids Res.* **2019**, *47*, D948−D954.
(59) Wang, D.; Gao, Y.; Liu, J.; Zheng, C.; Kong, X. Identifying drug−pathway association pairs based on L1L2,1-integrative penalized matrix decomposition. *Oncotarget.* **2017**, *8*, 48075−48085.
(60) Liu, J.; Wang, D.; Zheng, C.; Gao, Y.; Wu, S.; Shang, J. Identifying drug−pathway association pairs based on L2,1-integrative penalized matrix decomposition. *BMC Syst. Biol.* **2017**, *11*, 119.
(61) Wu, Z.; Peng, Y.; Yu, Z.; Li, W.; Liu, G.; Tang, Y. NetInfer: A Web Server for Prediction of Targets, Therapeutic and Adverse Effects via Network-Based Inference Methods. *J. Chem. Inf. Model.* **2020**, *60*, 3687−3691.

https://doi.org/10.1021/acs.jcim.1c00009
J. Chem. Inf. Model. 2021, 61, 2475−2485